

See discussions, stats, and author profiles for this publication at: <https://www.researchgate.net/publication/51165827>

Phylogeny, Adaptive Radiation, and Historical Biogeography in Bromeliaceae: Insights from an Eight-Locus...

Article *in* American Journal of Botany · May 2011

DOI: 10.3732/ajb.1000059 · Source: PubMed

CITATIONS

183

READS

290

19 authors, including:



Michael H J Barfuss

University of Vienna

37 PUBLICATIONS 1,137 CITATIONS

[SEE PROFILE](#)



Ralf Horres

GenXPro GmbH

40 PUBLICATIONS 1,175 CITATIONS

[SEE PROFILE](#)



Timothy M. Evans

Grand Valley State University

27 PUBLICATIONS 1,270 CITATIONS

[SEE PROFILE](#)



Georg Zizka

Goethe-Universität Frankfurt am Main and Sen...

271 PUBLICATIONS 1,798 CITATIONS

[SEE PROFILE](#)

Some of the authors of this publication are also working on these related projects:



Genetic Analysis of The Coffea Family [View project](#)



Phylojive [View project](#)

**PHYLOGENY, ADAPTIVE RADIATION, AND HISTORICAL
BIOGEOGRAPHY IN BROMELIACEAE: INSIGHTS FROM AN
EIGHT-LOCUS PLASTID PHYLOGENY¹**

THOMAS J. GIVNISH^{2,15}, MICHAEL H. J. BARFUSS³, BENJAMIN VAN EE^{2,4}, RICARDA RIINA^{2,5},
KATHARINA SCHULTE^{6,7}, RALF HORRES⁸, PHILIP A. GONSISKA², RACHEL S. JABAILY^{2,9},
DARREN M. CRAYN⁷, J. ANDREW C. SMITH¹⁰, KLAUS WINTER¹¹, GREGORY K. BROWN¹²,
TIMOTHY M. EVANS¹³, BRUCE K. HOLST¹⁴, HARRY LUTHER¹⁴, WALTER TILL³,
GEORG ZIZKA⁶, PAUL E. BERRY⁵, AND KENNETH J. SYTSMAN²

²Department of Botany, University of Wisconsin-Madison, Madison, Wisconsin 53706 USA; ³Department of Systematic and Evolutionary Botany, Faculty of Life Sciences, University of Vienna, Vienna A-1030, Austria; ⁴Department of Organismic and Evolutionary Biology, Harvard University, Cambridge, Massachusetts 02183 USA; ⁵Department of Ecology and Evolutionary Biology, University of Michigan, Ann Arbor, Michigan 48109 USA; ⁶Department of Botany and Molecular Evolution, Research Institute Senckenberg and J. W. Goethe University, Frankfurt am Main D-60325, Germany; ⁷Australian Tropical Herbarium, James Cook University, Cairns QLD 4878, Australia; ⁸GenXPro, Frankfurt am Main 60438 Germany; ⁹Department of Biological Sciences, Old Dominion University, Norfolk, Virginia 23529 USA; ¹⁰Department of Plant Sciences, University of Oxford, Oxford OX1 3RB, UK; ¹¹Smithsonian Tropical Research Institute, Balboa, Ancon, Republic of Panama; ¹²Department of Botany, University of Wyoming, Laramie, Wyoming 82071 USA; ¹³Department of Biology, Grand Valley State University, Allendale, Michigan 49401 USA; and ¹⁴Marie Selby Botanical Gardens, Sarasota, Florida 34236 USA

- **Premise:** Bromeliaceae form a large, ecologically diverse family of angiosperms native to the New World. We use a bromeliad phylogeny based on eight plastid regions to analyze relationships within the family, test a new, eight-subfamily classification, infer the chronology of bromeliad evolution and invasion of different regions, and provide the basis for future analyses of trait evolution and rates of diversification.
- **Methods:** We employed maximum-parsimony, maximum-likelihood, and Bayesian approaches to analyze 9341 aligned bases for four outgroups and 90 bromeliad species representing 46 of 58 described genera. We calibrate the resulting phylogeny against time using penalized likelihood applied to a monocot-wide tree based on plastid *ndhF* sequences and use it to analyze patterns of geographic spread using parsimony, Bayesian inference, and the program S-DIVA.
- **Results:** Bromeliad subfamilies are related to each other as follows: (Brocchinioideae, (Lindmanioideae, (Tillandsioideae, (Hechtioideae, (Navioideae, (Pitcairnioideae, (Puyoideae, Bromelioideae)))))). Bromeliads arose in the Guayana Shield ca. 100 million years ago (Ma), spread centrifugally in the New World beginning ca. 16–13 Ma, and dispersed to West Africa ca. 9.3 Ma. Modern lineages began to diverge from each other roughly 19 Ma.
- **Conclusions:** Nearly two-thirds of extant bromeliads belong to two large radiations: the core tillandsioids, originating in the Andes ca. 14.2 Ma, and the Brazilian Shield bromelioids, originating in the Serro do Mar and adjacent regions ca. 9.1 Ma.

Key words: Andes; Bromeliaceae; bromeliads; epiphytes; Guayana Shield; historical biogeography; neotropics; Poales; Serra do Mar; tank formation.

¹Manuscript received 13 February 2010; revision accepted 9 February 2011.

The authors gratefully acknowledge financial support for this investigation by grants from the National Science Foundation to P.E.B., K.J.S., and T.J.G. (DEB-9981587), T.J.G. (DEB-0830036), K.J.S. (DEB-0431258), and G.L.B. and T.M.E. (DEB-0129446 and DEB-0129414), and from the Hertel Gift Fund to T.J.G., from the Commission for Interdisciplinary Ecological Studies (KIÖS) at the Austrian Academy of Sciences (ÖAW, 2007-02 to W.T. and M.H.J.B., and from the Deutsche Forschungsgemeinschaft (ZI 557/7-1, SCHU 2426/1-1) and the Hessian initiative for the development of scientific and economic excellence (LOEWE) at the Biodiversity and Climate Research Centre, Frankfurt am Main, to G.Z. and K.S. Plant material was kindly supplied by the Selby Botanical Garden, the Palmengarten Frankfurt am Main, and the Botanical Gardens of Heidelberg. Alejandra Gandolfo provided some useful references on the geological history of the Andes. Many thanks to two anonymous reviewers and D. E. Soltis for several helpful suggestions.

¹⁵Author for correspondence (e-mail: givnish@wisc.edu)

doi:10.3732/ajb.1000059

The family Bromeliaceae (58 genera, ca. 3140 species) constitute one of the most morphologically distinctive, ecologically diverse, and species-rich clades of flowering plants native to the tropics and subtropics of the New World (Fig. 1). Bromeliads range from mist-shrouded tepuis in Venezuela to sun-baked granitic outcrops of the Brazilian Shield, from cloud forests in Central and South America to the cypress swamps of the southern United States, and from the frigid Andean puna to the arid Atacama (Smith and Downs, 1974; Givnish et al., 1997; Benzing 2000). Their distinctive leaf rosettes often impound rainwater in central tanks, possess the CAM photosynthetic pathway, and bear absorptive trichomes, providing mechanisms to weather drought and obtain or conserve nutrients on rocks and exposed epiphytic perches (Pittendrigh, 1948; McWilliams, 1974; Crayn et al., 2004; Givnish et al., 2007; Schulte et al., 2009). Bromeliad tanks also house a great diversity of insects—including some with substantial impact on human health—and other arthropods, as well as crabs, frogs, salamanders, and snakes.

In a hectare of cloud forest, these tanks can sequester tens of thousands of liters of rainwater and trap hundreds of kilograms of humus high in the canopy and provide key food sources for many primates and birds (Paoletti et al., 1991; Leme, 1993; Sillett, 1994; Richardson, 1999; Benzing, 2000; Acevedo et al., 2008). Some tank bromeliads are directly carnivorous (Fish, 1976; Frank and O'Meara, 1984; Givnish et al., 1984, 1997), and at least one is known to benefit from the prey captured by inquiline spiders (Romero et al., 2006). Many tank bromeliads are protected and/or fed by ants (Benzing, 1970, 2000; McWilliams, 1974; Givnish et al., 1997). Pollinators include a wide variety of insects, as well as hummingbirds, bats, and a few perching birds (Benzing, 1980, 2000; Luther, 1993; Beaman and Judd, 1996; Smith and Till, 1998; Buzato et al., 2000; Krömer et al., 2006; Tschapka and von Helversen, 2007). The inflorescences of *Puya raimondii* are the most massive of any flowering plant, while those of some dwarf *Brocchinia* and *Tillandsia* are only a few centimeters in height (Fig. 1). Finally, bromeliads contribute a large share of the total species richness of vascular epiphytes in neotropical forests, are particularly diverse at mid-elevations, and exhibit increasingly narrow endemism at higher elevations (Kessler, 2001; Krömer et al., 2005; Linares-Palomino et al., 2009; Linares-Palomino and Kessler, 2009).

To understand the genesis of these patterns—and, more generally, the history of adaptive radiation and geographic diversification in bromeliads—we need a well-resolved, strongly supported phylogeny for this remarkable family. Progress toward this goal initially was slow, partly because bromeliads are taxonomically isolated, with no clear outgroup with which to polarize character-states (Gilmartin and Brown, 1987; Terry et al., 1997; Givnish et al., 2000; Pires and Sytsma, 2002); partly because bromeliad plastid DNA evolves at an unusually slow rate (Gaut et al., 1992, 1997; Givnish et al., 2004, 2005); and partly because previous studies had limited taxon sampling.

Over the last dozen years, however, these roadblocks have been mostly overcome, through a greater understanding of relationships among monocot families overall (Givnish et al., 2005; Chase et al., 2006; Graham et al., 2006) and, within Bromeliaceae, through the sequencing and analysis of one or a few rapidly evolving genes and gene spacers in the plastid genome by individual laboratories (e.g., Terry et al., 1997; Horres et al., 2000; Crayn et al., 2004; Givnish et al., 2004, 2007; Sass and Specht, 2010). Based on a thorough sampling of taxa in all three traditional subfamilies—especially the critical Pitcairnioideae (characterized by winged or unappendaged seeds)—Givnish et al. (2007) presented the most comprehensive view of bromeliad phylogeny and evolution to date, based on cladistic analyses of sequences of the plastid gene *ndhF* and calibration of the resulting molecular tree against the known ages of several monocot fossils. Their findings placed *Brocchinia*, then *Lindmania* at the base of the bromeliad family tree, sister to all other taxa. The upper branches of that tree consisted of a trichotomy including *Hechtia*, the subfamily Tillandsioideae (characterized by plumose seeds), and a “ladder” consisting of four clades embracing all other bromeliads, including *Puya* (part of the traditional Pitcairnioideae) as sister to Bromelioideae (characterized by fleshy fruits) (Fig. 2). Using this phylogeny, Givnish et al. (2007) erected a new, eight-subfamily classification for bromeliads, splitting the traditional but highly paraphyletic Pitcairnioideae into Brocchinioideae, Lindmanioideae, Hechtioideae, Navioideae, Pitcairnioideae s.s., and Puyoideae (Fig. 2). The *ndhF* phylogeny resolved more of the higher-level relationships in Bromeliaceae than studies including fewer genera based on *ndhF* (Terry et al.,

1997), the *trnL* intron (Horres et al., 2000), or *matK* and *rps16* (Crayn et al., 2004), but was otherwise consistent with the results of those investigations. It also provided several new insights into the historical biogeography and adaptive radiation of bromeliads. However, the *ndhF* phylogeny provided only weak support for several nodes, failed to resolve the branching sequence of Tillandsioideae and Hechtioideae, and had a limited density of taxon sampling, including only 26 of 58 currently recognized genera, and none of the critical Chilean species of *Puya* (Jabaily and Sytsma, 2010) or Bromelioideae (Schulte et al., 2009).

To overcome these weaknesses, provide the basis for a more rigorous analysis of bromeliad evolution, and tap the wealth of data already in hand for several plastid loci—including those used to construct emerging, multilocus phylogenies for Bromelioideae (Schulte et al., 2005, 2009; Horres et al., 2007; Schulte and Zizka, 2008; Sass and Specht, 2010) and Tillandsioideae (Barfuss et al., 2005)—we formed an international consortium to produce a well-resolved, strongly supported phylogeny for Bromeliaceae based on multiple plastid loci and as comprehensive a sampling of bromeliad genera as could be managed.

Here we present the first results of that collaboration. To reconstruct relationships across Bromeliaceae, we completed the sequencing of eight rapidly evolving plastid regions for representatives of 46 of 58 bromeliad genera. We then used the resulting phylogeny to (1) analyze relationships within the family and test the new eight-subfamily classification, (2) infer the timing of divergence of various clades and relate these dates to events in Earth history, and (3) determine the geographical origins of the family and patterns of subsequent spread outside this region by members of each subfamily. A companion paper will calculate the rate of net species diversification for each major bromeliad clade and relate the observed differences in diversification rate to differences among clades in morphology, ecology, geographic distribution, mode of seed dispersal, and time of adaptive radiation.

MATERIALS AND METHODS

DNA extraction, taxon sampling, and selection of molecular markers—

Total genomic DNAs were extracted using the protocols of Crayn et al. (2004), Barfuss et al. (2005), Schulte et al. (2005), and Givnish et al. (2007). We sequenced eight rapidly evolving plastid regions (*atpB-rbcL*, *matK*, *ndhF*, *psbA-trnH*, *rpl32-trnL*, *rps16*, *trnL* intron, *trnL-trnF*) for 90 bromeliad species representing 46 genera, and three outgroups from Rapateaceae and Typhaceae (Appendix 1). An 81-gene analysis of relationships among monocot families (Givnish et al., 2010) placed Bromeliaceae sister to all other families of the order Poales, with Typhaceae being sister to all families of Poales except itself and Bromeliaceae, and Rapateaceae being sister to the remaining families of Poales. We used *Phoenix dactylifera* (Arecaceae) as the ultimate outgroup and downloaded sequences for all eight plastid regions for this species from the complete plastome sequence posted on GenBank.

Multiple species of *Aechmea*, *Mezobromelia*, *Navia*, *Ochagavia*, *Tillandsia*, and *Vriesea* were sampled due to concerns about the monophyly of those genera (Crayn et al., 2004; Barfuss et al., 2005; Schulte et al., 2005; Sass and Specht, 2010). Multiple species of *Brocchinia*, *Guzmania*, *Hechtia*, *Pitcairnia*, and *Puya* were included to help resolve the critical taxonomic positions of those genera. We included representatives of all genera of Brocchinioideae, Lindmanioideae, Tillandsioideae, Hechtioideae, Pitcairnioideae, and Puyoideae, all but one genus (*Steyerbromelia*) of Navioideae, and all but 11 of 34 genera of Bromelioideae (including 33 listed by Butcher 2008 and Luther 2008, and retaining *Pseudananas*). Of the 11 genera omitted, seven (*Androlepis*, *Fernseea*, *Hohenbergiopsis*, *Neoglaziovia*, *Orthophytum*, *Portea*, *Ursulaea*) were included in recent multilocus studies of relationships within Bromelioideae, and all were placed in that subfamily by plastid and nuclear data (Schulte and Zizka, 2008; Schulte et al., 2009; Sass and Specht, 2010). Genera not represented in this study include less than 2.5% of all described bromeliad species (see Luther, 2008). Subfamilial nomenclature follows Givnish et al. (2007).

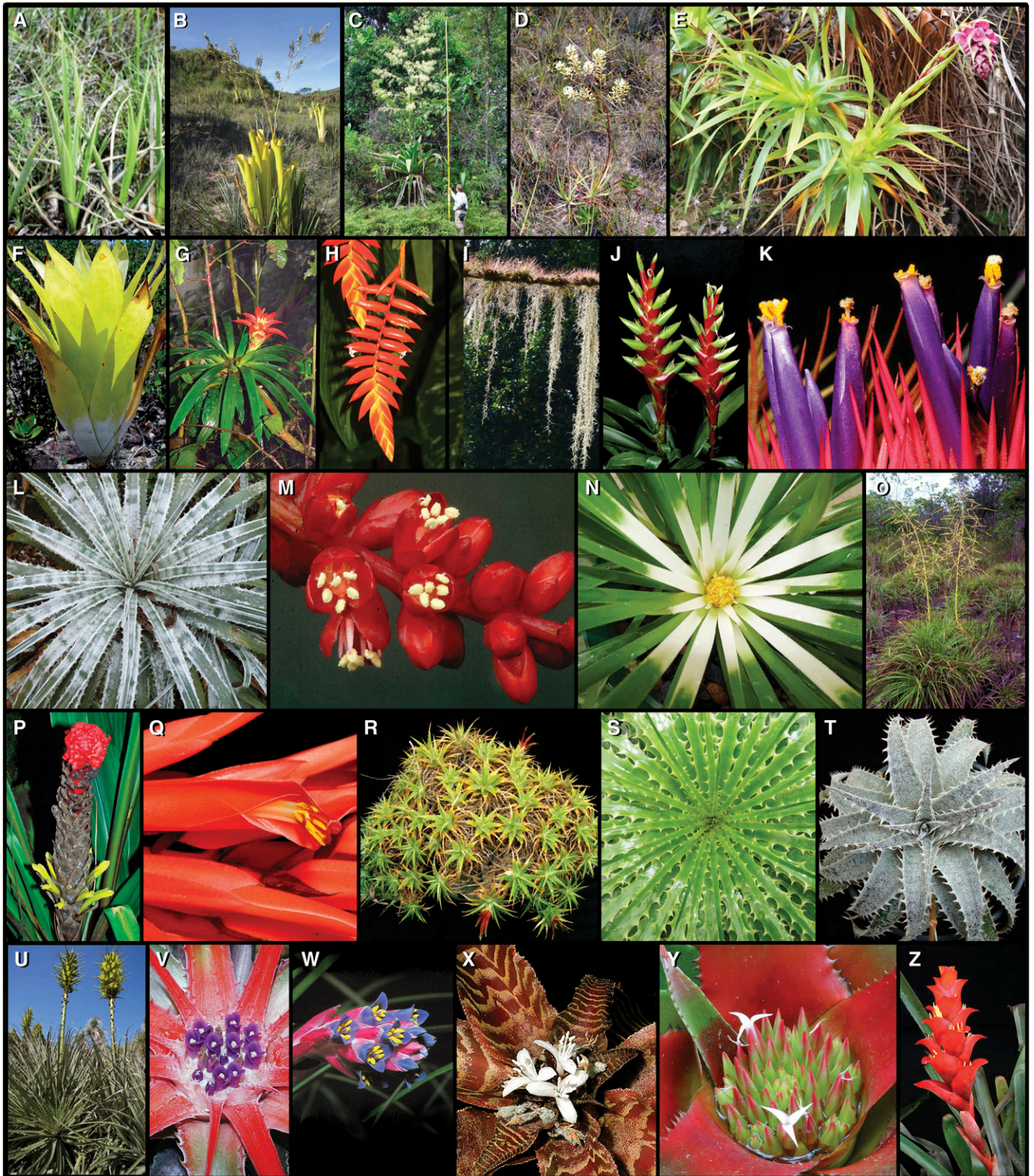


Fig. 1. Representative species of bromeliad subfamilies; images are at different scales. BROCCHINOIDEAE: (A) *Brocchinia prismatica*, nonim-pounding species sister to all *Brocchinia*, found in wet, sandy savannas in SW Venezuela; (B) *B. reducta*, terrestrial carnivore of damp, sandy savannas in SE Venezuela and SW Guyana; (C) tree-like *B. micrantha*, SE Venezuela and SW Guyana. LINDMANIOIDEAE: (D) *Lindmania guianensis*, SE Venezuela and SW Guyana; (E) *Connellia augustae*, sandstone outcrops, Venezuela and Guyana. TILLANDSIOIDEAE: (F) *Catopsis berteroniana*, carnivorous epi-phyte, Florida to Brazil; (G) *Guzmania lingulata*, epiphyte, Central and N South America; (H) *Tillandsia dyeriana*, epiphyte, Ecuador; (I) *Tillandsia seta-cea* (above branch) and *T. usneoides* (Spanish moss, below branch), widespread atmospheric epiphytes; (J) *Vriesea heliconioides*, epiphyte, Mexico to

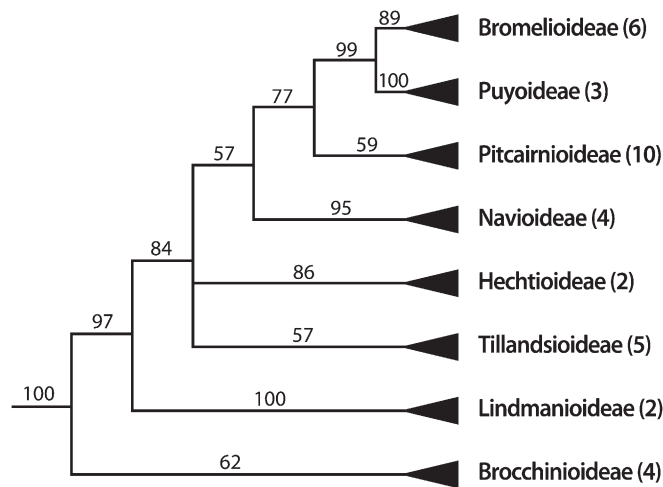


Fig. 2. Maximum-parsimony strict consensus tree from Givnish et al. (2007) based on variation in plastid *ndhF* sequences, with proposed relationships among bromeliad subfamilies. Outgroups from seven families of order Poales not shown. Numbers above branches are bootstrap support values; numbers in parentheses after subfamilial names indicate the number of taxa included in the earlier analysis.

We believe that our approach to higher-level bromeliad phylogenetics, based solely on sequences from the plastid genome, is justified because very few natural cases of hybridization among bromeliads are known, based on morphology or on more decisive comparisons of organellar vs. nuclear DNA markers (Wendt et al., 2008; Gonçalves and de Azevêdo-Gonçalves, 2009). Partly this may be because nuclear ribosomal ITS—the nuclear locus used to screen for hybridization and/or introgression in many angiosperm lineages—has only rarely been amplified and sequenced in bromeliads, given its strong hairpin geometry in this group (T. M. Evans, personal communication). However, Schulte et al. (2009), Gonsiska (2010), Jabail and Sytsma (2010), and Sass and Specht (2010), employing other nuclear markers (*PhyC*, *PRK*, and nrDNA ETS) with plastid sequences to evaluate relationships among hundreds of species, have identified only a very small number of putative hybrids, most notably the ancestor of the Chilean clade of *Puya* and one species of *Catopsis*. Thus, here we rely on multiple loci from the plastome genome to reconstruct evolutionary relationships, recognizing that the validity of our plastid phylogeny should be tested when it becomes possible to sequence and align low-copy nuclear genes across all subfamilies.

DNA amplification, sequencing, and alignment—Methods for amplifying and cycle-sequencing different plastid regions from total DNA extracts followed Barfuss et al. (2005) for *atpB-rbcL* and *rps16*; Crayn et al. (2004) for *matK*; Givnish et al. (2007) for *ndhF*; Horres et al. (2000, 2007) for the *trnL* intron and *trnL-trnF*; and Shaw et al. (2007) for *psbA-trnH* and *rpl32-trnL*. Sequences were visually aligned following Baum et al. (1994). Stretches of DNA that were difficult to align (i.e., there were multiple conflicting alignments possible under the assumptions of Baum et al.) or had missing data for a substantial number of taxa were excluded from analysis. We were unable to complete 60 (9.2%) of 651 sequences. GenBank accession numbers were acquired for all new sequences; previously obtained sequences were downloaded from GenBank (Appendix 1). An aligned data set has been deposited in

TreeBase (<http://www.treebase.org/treebase-web/home.html>; accessed 04-07-11), together with the maximum likelihood and Bayesian trees as case S11152.

Phylogenetic analyses—We inferred relationships from the nucleotide data using maximum parsimony (MP), maximum likelihood (ML), and Bayesian inference (BI). MP analyses were conducted using the program PAUPRat (Sikes and Lewis, 2001), based on Parsimony Ratchet (Nixon, 1999) and implemented in the Cyberinfrastructure for Phylogenetic Research (CIPRES) portal 2 teragrid (<http://www.phylo.org>) (Miller et al., 2010). Individual bases were considered multistate, unordered characters of equal weight; unknown nucleotides were treated as uncertainties. Following Nixon (1999) and Goloboff (1999), we performed multiple (50) independent searches in PAUPRat to cover tree space adequately. Each search involved 500 iterations, with the shortest trees from each search used to form a strict consensus tree and a majority-rule tree. Shortest trees from each successive search were combined with previous search trees to evaluate whether the combined search consensus tree had stabilized. Stabilization of a consensus tree based on multiple, independent searches in PAUPRat supports the accuracy of the topology obtained (Goloboff, 1999). We used bootstrap analysis (Felsenstein, 1985) in the program PAUP* 4.0b10 (Swofford, 2002) to assess the relative support for each node in the strict consensus, using 1000 random resamplings of the data and retaining 200 trees per iteration. To determine the extent to which the lower support for the monophyly of Puyoideae and Bromelioideae in this study vs. Givnish et al. (2007) was due to our inclusion here of a number of Chilean *Puya* and Chilean bromelioids and *Deinacanthon* of the nearby Gran Chaco, respectively, we removed the latter from the analysis and recalculated support values for Puyoideae and Bromelioideae. Consistency indices, including autapomorphies (CI) and excluding them (CI'), were calculated to evaluate the extent of homoplasy in the data (Givnish and Sytsma, 1997). Maximum-parsimony phylogenies were also formed for each plastid region, and incongruence length difference (ILD) tests (Farris et al., 1994) were conducted for each pair of regions (*ndhF*, *matK*, *trnL-trnF*, *atpB-rbcL*, *psbA-trnH*, *rpl16*, *rpl32-trnL*) in PAUP* after removing taxa not sequenced for either region, to assess potential conflicts between regions in phylogenetic structure.

Maximum-likelihood analyses used the program jModelTest 0.1.1 (Posada, 2008) based on the program PhyML (Guindon and Gascuel, 2003) to select the appropriate model of nucleotide evolution using the Akaike information criterion (AIC) (Posada and Buckley, 2004). We evaluated models for each of the plastid regions separately and the entire concatenated sequence. The most likely tree was produced using the program GARLI (Genetic Algorithm for Rapid Likelihood Inference; Zwickl, 2006) in CIPRES. Multiple models for each gene partition are not allowed in GARLI, so the more complex model for a given set of genes was chosen. Maximum-likelihood bootstrapping (MLB) was completed using the program RAxML 7.0.4 (Stamatakis et al., 2005, 2008).

Bayesian inference was performed in the program MrBayes 3.1 (Ronquist and Huelsenbeck, 2003) allowing different models for each region. Four independent runs of 5 000 000 generations each were completed with a chain temp of 0.2. Trees were sampled every 1000 generations. The first 25% of runs were discarded as burn-in. A majority rule consensus of the remaining trees from the four runs was produced in PAUP* 4.0 and used as the Bayesian inference tree with posterior probabilities (PP). We also explored the mixture model of Pagel and Meade (2008) as implemented in the program BayesPhylogenies (Pagel and Meade, 2004). This model allows the fit of more than one model of evolution to each site in the alignment. We used the recommended GTR + Γ model with "patterns=2, pi=true", allowing two rate matrices to be formed and allowing both rate parameters and base frequencies to vary.

Dating radiations—An indirect approach to calibrating the bromeliad phylogeny is required because almost all bromeliads occur in habitats that are poor

← Bolivia; (K) *Tillandsia ionantha*, flowers of tiny atmospheric epiphyte, Central America. HECHTIOIDEAE: (L) *Hechtia mooreana*, CAM terrestrial, Mexico; (M) partial inflorescence, *H. rosea*, CAM terrestrial, Mexico. NAVIOIDEAE: (N) *Navia* aff. *lactea*, saxicole, S Venezuela; (O) *Sequencia serrata*, E Colombia. PITCAIRNIOIDEAE: (P) *Pitcairnia holstii*, low-elevation terrestrial, Venezuela; (Q) bird-pollinated flowers, *P. undulata*, Mexico; (R) *Deuterocohnia lotteae*, high-elevation Andean cushion plant, S Bolivia; (S) *Encholirium spectabile*, CAM terrestrial, NE Brazil; (T) *Dyckia lindevaldae*, CAM terrestrial, Brazil. TILLANDSIOIDEAE: (U) *Puya chilensis*, tall terrestrial, Chile, cultivated at the Huntington Botanical Garden. BROMELIOIDEAE: (V) *Bromelia macedoi*, CAM terrestrial, Brazil; (W) *Fernseea bocainensis*, SE Brazil; (X) *Cryptanthus fosterianus*, nonimponding CAM terrestrial, SE Brazil; (Y) *Neoregelia eleutheropetala* var. *bicolor*, CAM epiphyte with flowers emerging from tank, S tropical America; and (Z) *Canistrum alagoanum*, CAM epiphyte with flowers emerging from tank, SE Brazil. Photo credits: A, Thomas Givnish; B, Peggy Faucher; O, Julio Betancour; T, Reginaldo Baião; all others, Bruce Holst.

for fossil preservation. There is only one macrofossil clearly assignable to Bromeliaceae, from Costa Rica 36 million years ago (Ma) (Smith and Till, 1998), long after both existing estimates of the age of origin of Bromeliaceae based on molecular data (Givnish et al., 2004, 2007). Lemé et al. (2005) recently erected a new family for a bromeliad-like fossil (*Protananas lucenae*) from northeastern Brazil in limestone 100–110 Myr old. The authors report, however, that this taxon appears to be a nonbromeliad close to the base of order Poales.

We conducted two analyses to assess the timing of the rise of the bromeliad stem lineage within Poales and of the crown radiation of the family. First, building on previous monocot-wide analyses of relationships and fossil dating (Bremer, 2000; Givnish et al., 2000, 2005; Janssen and Bremer, 2004), we used *ndhF* sequences of 333 taxa of monocots (including 71 from Bromeliaceae) and the outgroup *Ceratophyllum* to build a monocot-wide phylogeny. The ML tree derived in GARLI using a model from jModelTest was used for subsequent fossil calibration. As *ndhF* alone does not have the power to resolve several key nodes, we constrained five areas of the monocot backbone based largely on the results of a recent monocot-wide study employing 81 plastid genes (Givnish et al., 2010). These constraints included (1) (Araceae, (Tofieldiaceae, all other Alismatales)); (2) (Liliales, (Asparagales + commelinids)); (3) (Dasypogonaceae, Arecaceae); (4) (Poales, (Commelinales, Zingiberales)); and (5) (Bromeliaceae, (Typhaceae, (Rapateaceae, all other Poales))). We used the Langley and Fitch (1974) method, as implemented in the program r8s (Sanderson 2004), to reconstruct divergence times on the ML tree with *Ceratophyllum* pruned off assuming a molecular clock and conduct a χ^2 test of rate constancy to test for significant deviation from clocklike evolution. Given the nonclocklike pattern of evolution observed, we converted the ML tree into ultrametric form using penalized likelihood (PL) in r8s (Sanderson, 2002, 2004), calibrated against monocot-wide fossils.

Six Cretaceous fossils were used to constrain the corresponding nodes as minimum ages (Janssen and Bremer, 2004; Givnish et al., 2005; Hesse and Zetter, 2007). The monocot root was fixed at 134 Ma (Bremer, 2000; Janssen and Bremer, 2004). Penalized likelihood smoothes local differences in the rate of DNA evolution on different branches, taking into account branch lengths and branching topology and assigning a penalty for rate changes among branches that are too rapid or frequent, based on a smoothness parameter. We used the cross-verification algorithm in r8s (Sanderson, 2004) to find the optimal value of the smoothness parameter, based initially on minimizing the sum of the squared deviations between the observed and expected branch lengths derived by jackknifing each branch (Sanderson, 2002). We varied the smoothness parameter from 10^0 to 10^3 in steps of 0.25 of the exponent. The optimal value of the smoothness parameter was validated using the check-gradient algorithm in r8s. We ran separate r8s analyses using a range of smoothness values near the optimum to examine the impact of different values on variation in the stem and crown age of Bromeliaceae and chose the final value of the smoothing parameter based on minimization of that variation within the window of values that yield similar, near-minimal sums of the squared deviations between observed and expected branch lengths (see above). To estimate uncertainties in node age due to uncertainties in the monocot-wide *ndhF* branching topology, we calculated the standard deviation of the estimated age for each node (including those within Bromeliaceae) by forming 100 bootstrap resamplings of the sequence data employing the program PHYLIP (Felsenstein, 1993) and then using these to calculate realized branch lengths of the original ML tree for each resampling. The optimal smoothness parameter obtained for the entire data set was used in calculations for each resampling.

Second, we conducted a detailed r8s analysis of the entire eight-locus Bromeliaceae data set (including *ndhF*) with *Rapatea* (Rapateaceae) and *Typha* and *Sparganium* (Typhaceae), as well as the ultimate outgroup *Phoenix* (Arecaceae). Although the monocot-wide *ndhF* phylogenetic and fossil-dating analyses included Bromeliaceae, the eight-locus data set is essential for obtaining a more finely resolved estimate of branching events and their timing within the family. The stem and crown dates of Bromeliaceae obtained from the fossil-calibrated *ndhF* monocot chronogram were used as fixed dates in r8s for the eight-locus ML tree after removing *Phoenix*. Due to the ambiguity of monophyly in *Puya* based on plastid data, but the compelling support for it from nuclear sequence data and morphology (Jabaily and Sytsma, 2010), we ran r8s analyses with *Puya* constrained to be monophyletic.

To estimate variation in node age due to uncertainties in the derived node dates of the eight-locus data set and in the *ndhF* stem and crown node dates, we performed three further analyses. First, we calculated the standard deviation of inferred age at each node via 100 bootstrap resamplings of the eight-locus data set. Second, we calculated the standard deviation of both the stem and crown nodal dates for Bromeliaceae based on 100 bootstrap resamplings of the monocot-wide *ndhF* data; this allowed us to generate of the mean \pm SD of the inferred

ages for both the stem and crown nodes based directly on fossil calibration. Given that variation in inferred node ages is a function of random variation in the ages of the set-dates independent of random variation in node ages due to uncertainty in the eight-locus phylogeny, an estimate of the total standard deviation of inferred age at the stem and crown nodes can be estimated as $SD_{total} = (SD_{set-dates}^2 + SD_{phylogenetic}^2)^{0.5}$ (see Givnish et al., 2009). Finally, to quantify any bias or degree of uncertainty resulting from using the stem and crown ages from the *ndhF* tree to calibrate the eight-locus tree, we regressed the stem and crown ages for several critical nodes (each subfamily; the core tillandsioids, *Navia/Brewcaria*, *Pitcairnia*, and the Brazilian Shield and epiphytic tank bromelioid clades [see Results]; Puyoideae + Bromelioideae; and Puyoideae + Bromelioideae + Pitcairnioideae) for the eight-locus tree on those for the *ndhF* tree, eliminating the stem age of Bromelioideae to avoid duplication.

We related the timing of inferred cladogenetic events to the times of uplift and dissection of the tepuis of the Guayana Shield, formation of the Amazon basin, uplift of the Andes and Brazil's Serra do Mar, and shifts in regional climate as estimated by a variety of geological, climatological, and biogeographic studies (e.g., Vasconcelos et al., 1992; Hoorn et al., 1995, 2010; van der Hammen, 1995; Amorim and Pires, 1996; Potter, 1997; Safford, 1999; Coltorti and Ollier, 2000; Gregory-Wodzicki, 2000; Auler and Smart, 2001; Behling and Negrelle, 2001; Wang et al., 2004; Grazziotin et al., 2006; Garzzone et al., 2008; Antonelli et al., 2009; Ehlers and Poulsen, 2009; Figueiredo et al., 2009). Special attention was paid to the stem and crown ages of each subfamily, the core tillandsioids (sister to *Catopsis* and *Glomeropitcairnia*), and the clade of tank species sister to *Acanthostachys* (the core bromeliads; see Schulte et al., 2009).

Historical biogeography—To reconstruct spatial patterns of geographic diversification within Bromeliaceae, we employed three contrasting methods and accompanying assumptions implemented in the programs Statistical Dispersal–Vicariance Analysis (S-DIVA; Yu et al., 2010), BayesTraits (Pagel and Meade, 2007), and MacClade 4.08 (Maddison and Maddison, 2005). Given that the stem lineage of the family is already known to extend back to the Cretaceous but with a far more recent crown radiation (Givnish et al., 2004, 2007), and that bromeliads are clearly capable of long-distance dispersal—for example, from South America to the Galápagos (*Racinaea insularis*, Tillandsioideae), the Juan Fernandez Islands (*Greigia berteroi* and *Ochagavia elegans*, Bromelioideae), and tropical West Africa (*Pitcairnia feliciana*, Pitcairnioideae); see Smith and Downs (1974, 1977, 1979) and Givnish et al. (2007)—any assumption about the relative importance of vicariance vs. dispersal in Bromeliaceae would be difficult to justify. Programs to evaluate geographic diversification either favor vicariance (e.g., dispersal–vicariance analysis [DIVA, Ronquist, 1996, 1997; and S-DIVA]) or allow any amount of dispersal between areas (e.g., Bayes-Traits or MacClade using BI and MP criteria, respectively). Explicit, model-driven analyses of geographic diversification are possible (Ree et al., 2005; Ree and Smith, 2008), especially in the context of well-known geological events (e.g., continental vicariance as in Clayton et al., 2009), but remain premature for examining diversification within and among areas of geologically complex South America.

To minimize some of the shortcomings inherent in DIVA (Nylander et al., 2008; Harris and Xiang, 2009; Kodandaramaiah, 2010), we instead used S-DIVA (Yu et al., 2010). DIVA optimizes distributions for each node by allowing vicariance but minimizing assumptions of dispersal and extinction. S-DIVA extends DIVA by permitting assessment of phylogenetic uncertainty by examining multiple trees (in our case, a random subset of post burn-in Bayesian trees), each of which may contain polytomies.

Ranges of terminal taxa were atomized into recognized areas of endemism largely following Givnish et al. (2007) and (except for fusion of all Andean regions) Antonelli et al. (2009), including (1) Guayana Shield; (2) Brazilian Shield (including the Serra do Mar and Serra da Mantiqueira, as well as the adjacent Phanerozoic deposits of the Horn of Brazil and the Rio de la Plata basin); (3) Amazonia; (4) Caribbean (including the coast of northern South America and the southeastern United States); (5) Central America (including semiarid southern Texas); and (6) tropical West Africa. Distributional data were drawn from Smith and Downs (1974, 1977, 1979). Following the recommendation of Ronquist (1996), terminal species representing higher taxa (i.e., genera) were scored for ancestral area where possible (specifically, for *Catopsis* in Central America [Gonsiska, 2010]). When that approach was not justified or feasible, we scored single placeholders for all portions of the generic range (e.g., *Bromelia*) despite the known sacrifice in geographical resolution at deeper nodes in S-DIVA reconstructions (Ronquist, 1996). Multiple species per genus were each scored based on their own distribution. Vicariance between the Guayana Shield and the Andes, Caribbean, and Central America were excluded, as was

vicariance between tropical West Africa and any other region, due to the lack of any geographic contact between these regions over the inferred age of the bromeliad stem group. Due to the ancient split of Bromeliaceae from all other Poales, we performed several iterations of S-DIVA with respect to different outgroups (i.e., Rapateaceae and Typhaceae). Rapateaceae (and other lineages among the early splits in Poales) are Guayanan, whereas Typhaceae are cosmopolitan. We thus ran S-DIVA with the two outgroup families scored as Guayana Shield and polymorphic, respectively. We also ran analyses after scored both outgroups as Guayana Shield, due to the strong signal of Guayana Shield as basal in more Poales-wide biogeographic analyses (Givnish et al., 2000, 2004, 2007). Last, we removed Typhaceae entirely as an outgroup, as advocated by Bremer (2002), who removed this aquatic, easily dispersed group in DIVA analysis because it would be dangerous to base any conclusions regarding ancestral distributions on their present distributions. A random subset of 1000 Bayesian posterior probability trees from the phylogenetic analysis of the eight-locus data set were input into S-DIVA to estimate probabilities of ancestral areas at each node. We explored the impact of restricting the number of unit areas allowed in ancestral distributions by using the maxareas option (all possible areas, 4, and 2). The ancestral areas for all nodes were visualized on the ML tree with *Puya* constrained to be monophyletic.

We also analyzed the biogeographical data using ML and MP reconstructions that relax emphasis on vicariance by permitting dispersal between any pair of biogeographic areas. We implemented BI optimization of ancestral areas (Pagel, 1999) with the Markov chain Monte Carlo (MCMC)-based Bayes-MultiState option in the program BayesTraits v.1.0 (Pagel and Meade, 2007) using the ML tree with *Puya* constrained to be monophyletic to portray ancestral area reconstructions. To reduce some of the uncertainty and arbitrariness of choosing priors under MCMC, we used the hyperprior approach (the rjhp command) as recommended (Pagel et al., 2004; Pagel and Meade 2007). Combinations of hyperprior values (exponential or gamma, mean and variance) and rate parameter values were explored to find acceptance rates when running the Markov chains of between 20 and 40% (as recommended by Pagel and Meade, 2007). All subsequent analyses used the reversible-jump hyperprior command (rjhp gamma 0 30 0 10) that seeded the mean and variance of the gamma prior from uniform hyperpriors on the interval 0 to 30 and 0 to 10, respectively, and a rate parameter of 150 (ratedev 150). We reconstructed ancestral areas using MP by overlaying the ranges of individual species (or inferred ancestral area for *Catopsis*) using MacClade 4.08 (Maddison and Maddison, 2005), resolving all of the most parsimonious states at each node of the ML tree.

RESULTS

Phylogeny—We obtained an aligned data matrix of 94 taxa × 9341 characters; of the latter, 1210 were parsimony-informative and 1429 were variable but parsimony-uninformative (Table 1). The number of informative characters varied nearly 6-fold among loci, from 61 for *psbA-trnH* to 357 for *ndhF*. The fraction of informative sites varied from 8.8% (*psbA-trnH*) to 16.2% (*rpl32-trnL*). The numbers of informative vs. variable but uninformative characters were strongly correlated with each other across loci ($r = 0.97$, $P < 0.0001$ for two-tailed t test with 6 df), and the ratio of informative to variable but uninformative characters averaged 0.85 ± 0.074 (mean \pm SD). Within Bromeliaceae, 1663 characters were variable, of which 766 were informative.

Maximum parsimony resulted in a single island of 1 317 600 trees of length 4546 steps, and a strict consensus tree that was well resolved outside subfamily Bromelioideae (Fig. 3). The consistency index CI for these trees was 0.70; CI' (excluding autapomorphies) was 0.54. Branches that were unusually short (see below) were usually lost in the strict consensus tree relative to the majority-rule tree (Fig. 3).

The MP strict consensus tree supported the monophyly of all eight proposed subfamilies; each had 99–100% bootstrap support except Puyoideae and Bromelioideae (Fig. 3). Chilean *Puya* formed a clade with 100% bootstrap support; non-Chilean *Puya* had 99% support. *Puya* as whole—while resolved as monophyletic—had less than 50% support (Fig. 3). Bromelioideae had 59% bootstrap support. *Bromelia*, *Fascicularia-Ochagavia*, *Deinacanthon*, and *Greigia* formed a weakly supported clade sister to all other bromelioids in the MP majority-rule tree and a basal polytomy in the strict consensus tree. *Pseudananas* is sister to the remaining bromelioids (61% bootstrap), then *Ananas*. A core group of bromelioids, sister to and including *Ananas*, had 88% bootstrap support, but seven of 24 relationships within this core group were unresolved in the strict consensus (Fig. 3). The clade consisting of Bromelioideae and Puyoideae had 100% bootstrap support.

Support levels for the monophyly of each of the eight subfamilies in the strict consensus tree were generally much higher than those in the original *ndhF* phylogeny (Figs. 2, 3), except for Puyoideae and Bromelioideae. Experimental removal of taxa show that these two subfamilies had lower support in the current analysis due to our inclusion of Chilean *Puya*, Chilean bromelioids, and *Deinacanthon* from the nearby Gran Chaco. Relationships among the eight subfamilies agreed with those in the original *ndhF* phylogeny (Fig. 2) but were better supported. In addition, the eight-locus data set resolved the subfamilial trichotomy present in the *ndhF* phylogeny, placing Hechtioideae sister to (Navioideae, (Pitcairnioideae, (Bromelioideae, Puyoideae))), and Tillandsioideae sister to all five subfamilies (Fig. 3).

In both the strict consensus and majority-rule trees, *Broccinia*, *Guzmania*, *Hechtia*, *Deuterocohnia*, *Dyckia*, *Encholirium*, *Fosterella*, *Pitcairnia*, *Puya*, *Ananas*, and *Araecoccus* emerged as monophyletic. In contrast, *Lindmania*, *Tillandsia*, *Navia*, and *Ochogavia* were paraphyletic; *Mezobromelia*, *Vriesea*, and especially *Aechmea* (with at least six apparent “origins”) were polyphyletic (Fig. 3). In the MP majority-rule tree, *Acanthostachys* was sister to taxa corresponding to the tank-bromelioid clade (“core bromelioids”) of Schulte et al. (2009) and its sister *Cryptanthus*; *Acanthostachys*, *Cryptanthus*, and the tank bromelioids formed an unresolved trichotomy in the strict consensus (Fig. 3).

MP trees based on individual plastid regions were less resolved and less well supported than the strict consensus phylogeny

TABLE 1. Numbers of parsimony-informative, variable but parsimony-uninformative, and invariant sites for each of the plastid regions sequenced, as well as the consistency indices (with and without autapomorphies) and proportion of informative sites for those regions.

Region:	<i>matK</i>	<i>ndhF</i>	<i>rps16</i>	<i>atpB-rbcL</i>	<i>psbA trnH</i>	<i>rpl32- trnL</i>	<i>trnL-trnF, trnL intron</i>	Total
No. informative sites	213	247	132	123	70	195	169	1149
No. variable but uninformative sites	200	310	151	145	71	251	170	1298
No. invariant sites	1218	1541	862	1109	759	937	808	7234
Total aligned bp	1631	2098	1145	1377	900	1383	1147	9681
Consistency index (CI)	0.70	0.71	0.72	0.66	0.69	0.72	0.73	0.71
CI'	0.56	0.54	0.57	0.49	0.55	0.56	0.59	0.55
Informative sites/base	0.131	0.118	0.115	0.089	0.078	0.140	0.141	0.119

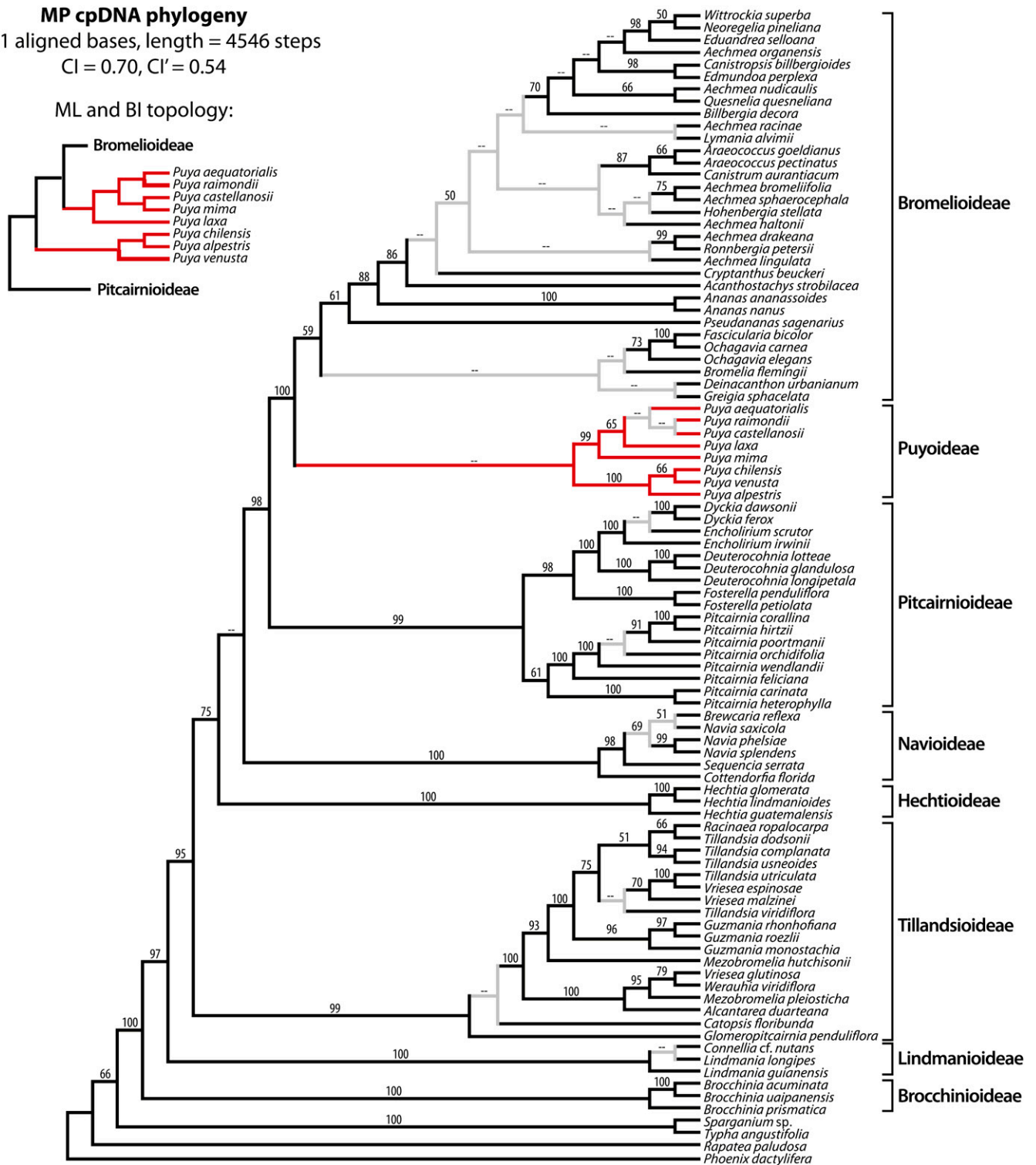


Fig. 3. Maximum-parsimony (MP) majority-rule phylogeny based on eight plastid loci; figure also shows the MP strict consensus tree, in which the light gray branches collapse. Numbers above branches are bootstrap support values; missing values indicate support less than 50%. Tree length = 4546 steps; CI = 0.70 and CI' = 0.54 excluding autapomorphies. *Puya* (red branches) is monophyletic in the MP tree, but paraphyletic in the maximum-likelihood (ML) and Bayesian inference (BI) trees (see inset).

based on the combined data set. Although ILD tests showed apparently significant differences in phylogenetic structure between some pairs of regions, such differences only occurred in

comparisons when one or both regions with relatively small numbers of phylogenetically informative sites (Table 1). Furthermore, for each region, the MP strict-consensus tree did not

diverge from the combined-data phylogeny at nodes well supported ($\geq 90\%$ bootstrap support) in the former.

For maximum-likelihood analysis, the AIC identified the optimal models as TVM + Γ for *ndhF*; TVM + I + Γ for *matK*, *trnL* (plus intron), *atpB*, and *rps16*; and GTR + I + Γ for *psbA-trnL* and *rpl32*. The maximum-likelihood and Bayesian trees were nearly identical to each other in topology and mostly congruent with the MP majority-rule tree, but placed Bromelioideae in a paraphyletic *Puya*, sister to the non-Chilean taxa (Figs. 3–5). Both ML and BI placed *Hechtia* sister to Navioideae-Pitcairnioideae-Puyoideae-Bromelioideae, congruent with the MP tree. Both placed *Catopsis* sister to *Glomeropitcairnia* at the base of the tillandsioids (Figs. 4, 5). The four areas of greatest phylogenetic uncertainty within bromeliads—as judged by differences in topology among trees or the degree of resolution within each tree—correspond to the portions of those trees with exceedingly short branch lengths, including (1) early-divergent bromelioids, (2) late-divergent bromelioids, (3) relationships among Chilean and non-Chilean *Puya*, and (4) relationships among *Catopsis*, *Glomeropitcairnia*, and all other tillandsioids (Figs. 3, 5). Conflicts among the three phylogenies generally did not occur at nodes that are well supported by each individually.

Molecular clocks and dating—Cross-verification of a penalized-likelihood calibration of the *ndhF* ML tree across monocots showed that smoothing parameters between 50 and 100 yielded very similar, nearly minimal sums of the squared deviations between the observed and expected branch lengths derived by jackknifing each branch. Within that range, a smoothing parameter of 75 minimized the variance in the apparent ages of the crown and stem node of Bromeliaceae. We used this value to calibrate the across-monocot tree, producing estimates of the bromeliad stem age as 100.0 ± 5.2 million years ago (Ma) (and the corresponding crown age as 19.1 ± 3.4 Ma (Fig. 6). These dates were then employed to calibrate the eight-locus bromeliad tree; cross verification produced a smoothness parameter of 100. The resulting chronogram (Fig. 7) resolved cladogenetic events within Bromeliaceae from 19.1 to 0.64 Ma. The standard deviation of estimated ages for individual nodes generally varied from 0.5 to 2 Myr, with smaller estimated amounts of variation due to phylogenetic uncertainty in nodes closer to the present (Fig. 7). Regression of estimated ages for several representative nodes in Bromeliaceae from the eight-locus tree on those from the across-monocots phylogeny (Table 2) yielded excellent agreement between the two sets of estimates ($y = 1.060x - 0.032$, $r^2 = 0.80$, $P < 0.0001$ for 25 df).

Historical biogeography—Reconstruction of ancestral areas using MP, BI, and S-DIVA generally agreed with each other, with the exception of a few nodes detailed below (Fig. 8). Based on our eight-locus chronogram and biogeographic reconstruction using MP, we infer that bromeliads arose in the Guayana Shield ca. 100 Ma, based on the restriction to this ancient craton—and in most cases, to highly leached marine sandstones of the overlying Precambrian Roraima Formation—of Brocchinioideae and Lindmanioideae, nested sequentially at the base of the family. Brocchinioideae diverged from the ancestor of all other bromeliads ca. 19.1 Ma, and extant species of *Brocchinia* began to diverge from each other ca. 13.1 Ma (Fig. 8). All other extant bromeliad subfamilies began diverging from each other slightly before that, with the stem lindmanioids diverging from the ancestor of other bromeliads ca. 16.3 Ma. The stem tilland-

sioids arose shortly after that, ca. 15.4 Ma (Fig. 8). Based on MP, it is unclear whether tillandsioids arose on the northern littoral of South America, in the Andes, or in Central America (Fig. 8). *Catopsis*, sister to *Glomeropitcairnia* with its sister to the remaining tillandsioids, today grows in the Guayana Shield as well as the north coast of South America, the Caribbean, Central America, and southern Florida, but appears to have arisen in Central America (Fig. 8). *Glomeropitcairnia* is endemic to the Lesser Antilles, Trinidad, and Tobago, and the north coast of Venezuela, and appears to have diverged from *Catopsis* about 14.0 Ma. The ancestor of the remaining members of the subfamily—which we term the core tillandsioids—appears to have arisen in the Andes about 14.2 Ma, with the modern genera beginning to diverge from each other ca. 8.7 Ma, with evolution mainly in the Andes but with several subsequent invasions of Central America, the northern littoral of South America, and the Caribbean (Fig. 8).

Hechtia arose ca. 16.6 Ma and invaded Central America independently (Fig. 8). Extant species of *Hechtia* began differentiating from each other ca. 10.3 Ma. About 15.0 Ma, Navioideae arose in the Guayana and/or Brazilian Shields, with restriction to the Guayana Shield after 10.4 Ma, corresponding to the endemism there of *Brewcaria*, *Navia*, and *Sequencia* and of *Cotendorfia* to the Brazilian Shield.

The common ancestor of the three remaining subfamilies evolved about 15.0 Ma in the Andes (Fig. 8), where *Pitcairnia* grows from near sea level to above treeline (with scattered occurrences elsewhere in the Guayana Shield and southeastern Brazil), *Fosterella* grows mostly at midelevations in mesic sites (with disjunct occurrences in Central America), *Dyckia* grows in drier sites from mid to high elevations and extends into the Brazilian Shield and the Rio de la Plata basin (including the Gran Chaco within the latter), and *Deuterocohnia* occurs as cushion plants in arid, high-elevation sites just south of the “knee” of the Andes, in southern Bolivia and northern Argentina (Fig. 9). Pitcairnioideae arose ca. 13.4 Ma; *Pitcairnia*, ca. 12.0 Ma; *Fosterella*, ca. 11.3 Ma; and *Deuterocohnia*, ca. 8.5 Ma. Based on the taxa included in this study, the lineage leading to *Pitcairnia feliciana* dispersed to Guinea in west Africa from the Andes sometime in the last 9.3 Myr. *Dyckia* and *Encholirium* (the latter restricted to northeastern Brazil) form a clade sister to *Deuterocohnia* and apparently invaded the Brazilian Shield from the Andes, beginning 8.5 Ma (Figs. 8, 9). Given the geographic overlap of *Deuterocohnia*, *Dyckia*, and *Fosterella* in south-central Bolivia (Fig. 9), it is likely that key cladogenetic events in Pitcairnioideae occurred there.

The common ancestor of *Puya* and the bromelioids arose about 13.4 Ma in the Andes (Fig. 8). Ancestral *Puya* diverged from the ancestral bromelioids ca. 10.1 Ma, with *Puya* splitting almost immediately (10.0 Ma) into two clades distributed in the Andes in low-elevation Chile vs. the rest of the cordillera at mid to high elevations. Present-day species of *Puya* began to diverge from each other during the last 3.5 Myr in the Andes, and during the last 2.5 Myr in Chile (Fig. 8). In the ML, BI, and MP majority-rule trees, a clade of five small bromelioid genera—mostly from Chile and the southern Andes—are sister to the remaining members of Bromelioideae (Fig. 8). Three of these genera (*Fascicularia-Ochagavia* and *Greigia*) are partly or wholly restricted to temperate regions at low elevations in the southern Andes, including low-elevation habitats just above high tide in *Fascicularia bicolor* and *Ochagavia litoralis* in continental Chile, and *O. elegans* in the Juan Fernandez Islands. *Greigia* grows in montane habitats from Central America to the Andes, and in the

ML phylogeny



Fig. 4. Maximum-likelihood (ML) phylogram for Bromeliaceae based on concatenated sequenced data. Branch lengths are proportional to the inferred number of nucleotide changes down each branch. *Puya* (red branches) is paraphyletic in the ML tree, but monophyletic in the MP tree.

understory of humid deciduous and evergreen forests in southern Chile and the offshore Juan Fernandez Islands. Two other genera—monotypic *Deinacanthon* and species-rich *Bromelia*—grow in the Gran Chaco (the southwestern portion of the Rio de la Plata basin, adjacent to the Andes) and throughout the Neotropics at low elevations, respectively (Fig. 8).

The remaining bromelioids form the “Brazilian Shield clade”, which arose in the Brazilian Shield ca. 10.1 Ma via dispersal from the Andes (Fig. 8). Members of this clade subsequently dispersed repeatedly outside this region, notably in *Ananas*,

Aechmea, *Araeococcus*, *Billbergia*, *Neoregelia*, and *Ronnbergia*, but most taxa are restricted to a narrow portion of the Brazilian Shield near the southeastern coast of Brazil, running ca. 1500 km from Minas Gerais to Rio Grande do Sol. This area includes the Brazilian Highlands (Serra do Mar and the more inland Serra da Mantiqueira) and adjacent coastal plain, with their extremely humid, highly diverse Atlantic rain forests and cloud forests, restingas on sandy soils, mangroves, campos de altitude, and drier vegetation inland (e.g., campos rupestres on rocky outcrops). The bromelioid tank-epiphyte clade—sister to